THE EFFECTS OF INTERELEMENT SPACING IN LINEAR ARRAYS ON THROUGHPUT PERFORMANCE IN AD HOC NETWORKS

Sonia Furman, David E. Hammers, and Mario Gerla
Electrical Engineering and Computer Science Departments, University of California, Los Angeles
Los Angeles, California 90095, U.S.A.

Keywords: Ad hoc networks, Sidelobes, Fading, Hidden nodes, Directional antennas, QualNet

Abstract: With the high demand for improved signal link quality in ad hoc networks, devices configured with omnidirectional antennas can no longer meet the growing needs in throughput performance, and alternative approaches using antenna arrays that provide directional radiation patterns are sought. This study models an 8-element linear antenna array and examines the effects of interelement spacing of the array on the ad hoc network's throughput performance. We show through simulation, that as a result of the antenna array, the throughput performance of the network consistently improved compared to that with an omnidirectional antenna. Interestingly, we determined that the maximum increase in performance of over 150% was attained with the smallest interelement spacing of 0.5λ rather than with the larger interelement spacing and higher gain. With null-steering, this performance increased even further to 180%.

1 INTRODUCTION

Attributes of ad hoc networks provide a powerful combination of both mobile access and configuration flexibility that enables fast deployment critical to military applications and recovery operations. Unlike cellular and radar communication systems, ad hoc networks are local area networks (LANs) that communicate over a medium with no observable boundaries, are formed without pre-planning, and exist only for as long as they are needed (IEEE 1999). The inherent features that make these networks so attractive are also those that bring a higher level of complexity to the design of protocols and transceivers. Although solutions to enhance link quality using antenna arrays have been employed extensively in other wireless communication systems, this approach has not yet been fully exploited in ad hoc networks and is still in its infancy stages. To employ antenna arrays in future devices associated with ad hoc networks, challenges concerning the physical (PHY) and medium access control (MAC) layers of the network need to be addressed. These challenges include modifying existing protocols associated with the IEEE 802.11 standards (IEEE 1999, 2000) that will accommodate effective beam steering policies, and designing accurate antenna array models that reflect realistic wireless channel conditions. Previous studies (Ko, Shankarkumar & Vaidyn 2000; Nasipuri el al. 2000; Ramanathan 2001), have shown the benefits of directional antennas (antenna arrays) in ad hoc networks by modifying MAC protocols that provide effective mechanisms for beam steering policies while using hypothetical antenna models on both the transmitter and receiver. This work like prior work, establishes the benefits of antenna arrays in an ad hoc networks, yet differs considerably from prior work in that it provides the design of accurate antenna array models employed only at the receiver, and determines through simulation the effects of interelement spacing of the array on the network's throughput performance.

In the remainder of this paper, Section 2 presents a summary on the benefits of directional antennas in ad hoc networks and discusses the implications on the hidden node problem. Section 3 describes the design of the linear antenna array with the three variants of interelement spacing. Section 4 discusses an analytical approach to maximize the SINR in a fading channel. Section 5 provides the ad hoc network environment used in the simulation and

Furman S., E. Hammers D. and Gerla M. (2004).
THE EFFECTS OF INTERELEMENT SPACING IN LINEAR ARRAYS ON THROUGHPUT PERFORMANCE IN AD HOC NETWORKS.
In *Proceedings of the First International Conference on E-Business and Telecommunication Networks*, pages 150-159
DOI: 10.5220/0001390701500159

the results obtained, followed by a summary with conclusions on the study in Section 6.

2 BENEFITS OF ANTENNA ARRAYS IN AD HOC NETWORKS

Benefits of antennas arrays in wireless ad hoc networks have gained much interest in recent years due to their potential to enhance network performance. In comparison to an omnidirectional antenna which produces an azimuthal radiation pattern of 360^o, the array produces a narrow beam in which the confined energy (or main lobe) is pointed in the direction of the desired signal resulting in a notable reduction in interference, and the ability to mitigate multipath, leading to improved channel capacity and spectrum efficiency. Channel capacity is a measure that describes the maximum data rate in a channel of designated bandwidth (Blogh & Hanzo 2002), and improved channel capacity (or spectrum efficiency) implies the support of more users within that bandwidth without loss of throughput performance. Omnidirectional antennas are among the primary contributors to limiting channel capacity and spectrum efficiency in ad hoc networks, thereby creating a need for researchers to identify alternative solutions and new approaches in the design of the PHY layer.

Researchers suggest that there are substantial performance improvements in throughput and packet delay to be gained by employing directional antennas in ad hoc networks. Ko, Shankarkumar, and Vaidyn (2000) have shown that the bandwidth efficiency and throughput performance increased with an abstract directional antenna due to their design of a medium access control protocol D-MAC. Nasipuri et al (2000) also proposed a modified MAC protocol to control a hypothetical 4-directional antenna model at both the transmitter and receiver for which the average throughput in the network increased by 2 to 3 times compared to that with an omnidirectional antenna. In a comprehensive study on the performance of ad hoc networks with approximate antenna patterns, results in throughput improvement of 28-118% depending on network density have been reported (Ramanathan 2001). A 72% throughput improvement has been documented in (Sanchez, Giles &. Zander 2001) by utilizing 60^o beamwidth antennas in an ad hoc network using a specific beam selection policy. These observations for the most part relied on modified MAC protocols that provided additional attributes to accommodate beamsteering routines for systems that incorporate abstract antenna arrays, at both the transmitter and receiver (Ko, Shankarkumar & Vaidyn 2000; Nasipuri el al. 2000). In our work it was not necessary to modify the MAC protocol but instead we relied on the simulators ability to steer the beam. From our array model, 24 beams were generated (eight beams per each of the 3 variants of interelement spacing), and tabulated in terms of gain per 1^o increments (through 360^o), to perform the simulation in all the scenarios.

A unique characteristics that continues to perplex researchers in ad hoc networks, is that of the hidden node problem. Of particular interest is the effect of antenna arrays on the spectrum efficiency of the network, subject to the hidden node problem. The hidden node (terminal) problem has been known to have an adverse effect on ad hoc networks performance primarily due to access restrictions inherent in the IEEE 802.11 MAC protocol (Khurana, Kahol & Jayasumana 1998; Hadzi-Velkove & Gavrilovska, 1999), where it is assumed to be configured with an omnidirectional antenna. The inefficiencies in communications that arise due to the hidden node problem, and the potential increase in performance attributed to the antenna array are described below.

The scenario in which the hidden node problem arises is when a transmitter outside the radio range of a transmitting node is not aware of its neighboring node receiving, and attempts to transmit, causing interference or a garbled message. Peterson and Davie (2000) define the hidden node problem as a "…situation that occurs on a wireless network where two nodes are sending to a common destination, but are unaware that the other exists". Figures 1(a) through 1(d) attempts to capture the hidden node problem with an omnidirectional antenna. The circles represent the radio range of the nodes A, B, C and D. We assume that all nodes have equal radio range. In Figure 1(a), we assume that nodes A & C attempt to send a message to node B at about the same time. Node C does not know that A is attempting to send to node B since A is hidden from node C (C is out of radio range with A – *'dashed line*'), and therefore a situation of collision arises.

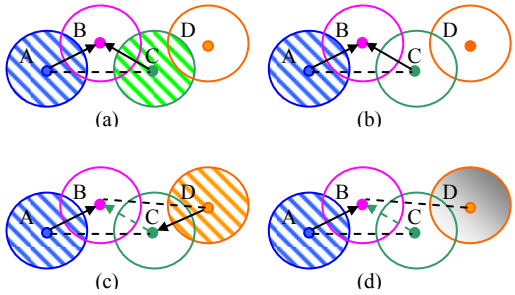

Figure 1: Hidden node problem with omnidirectional antenna

This collision occurred in spite of the MAC protocol designed to send and receive short control frames, Ready-To-Send/Clear-To-Send/Acknowledge (RTS/CTS/ACK), to ensure collision avoidance in the multiaccess scheme Carrier Sense Multiple Access with Collision Avoidance (CSMA/CA). In Figure 1(b), both A & C are attempting to connect to B at slightly different times. Node A succeeds in establishing communication with B, thereby blocking C from transmitting or receiving. Note that this time only the A circle is filled since it is the only node transmitting, and since C is blocked it remains quiet for the duration of the transmission between A & B. In Figure 1(c), node D wants to send information to C since it cannot detect that the channel is busy, i.e. B is not within radio range of D (*broken line between B and D*). Potentially, D may transmit but not to node C because C is blocked on behalf of B that is receiving from node A (*B is within radio range of C*). In Figure 1(d), node D unnecessarily has to wait to transmit to C at least until node A completes its transmission to B, which clearly is inefficient and undesirable. These inefficiencies have been quantified in various studies (Khurana, Kahol & Jayasumana 1998; Hadzi-Velkove & Gavrilovska, 1999). Moreover, it has been shown that the throughput consistently declined as the probability of hidden nodes increased (Hadzi-Velkove & Gavrilovska 1999). Khurana, Kahol & Jayasumana (1998) have shown through simulation that throughput is acceptable when the number of hidden pairs is less than 10%, but then degrades significantly when the number of hidden pairs increases.

Figure 2 suggests that by using an antenna array in the above network access scenarios, the throughput will increase significantly. In Figure 2, nodes A & B perform the RTS\CTS\ACK handshake, using omnidirectional communication. B goes into the receive data mode with a directional

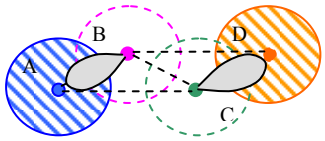

Figure 2: Increased network capacity with directed beams from antenna array

antenna pointed at A. We repeat the scenario for Figure 1(c) where D wants to transmit to C. In this case, once B is in the receive mode, C is no longer blocked to receive, and D may transmit to C as long as B is receiving from A but not transmitting to A. Node C, using a directional beam may now receive from D without creating interference to B even though C is in radio range of B. Using directional beams in the network, the 2 additional nodes (C & D) which otherwise may have been blocked, or have been in a wait mode like node D in Figure 1(d) are now able to communicate compared to only 2 nodes communicating in Figure 1. This example clearly demonstrates the potential of an antenna array to increase network capacity and spectrum efficiency in an ad hoc network.

3 SYNTHESIS OF THE LINEAR ARRAY

Antenna synthesis in its simplest form is a methodic process whereby a radiation pattern defined in terms of its main beam and sidelobes is obtained from a specific antenna configuration in which the hardware design constraints (current, coupling, etc.) of the antenna are satisfied. Figure 3 summarizes the parameters associated with antenna synthesis. Synthesis methods for the most part rely on the relationship between the excitation current of the array and the pattern generated.

In our design, we used these parameters as a

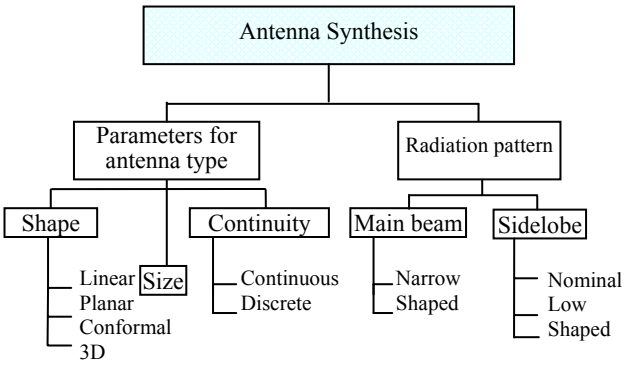

Figure 3: Antenna synthesis parameters

guide to generate radiation patterns for narrow main beams and low sidelobes with an antenna type of a linear array shape (Figure 4). The desired normalized radiation pattern $F(\theta,\phi)$ of a linear array with parallel uncoupled elements (along the x-axis) is defined in (1) as the product of the element pattern of the array $g_a(\theta,\phi)$, and the array factor $f(\theta,\phi)$ (Stutzman & Thiele 1998).

$$F(\theta,\phi) = g_a(\theta,\phi) f(\theta,\phi) \quad (1)$$

where: θ and ϕ are the elevation and azimuthal angle respectively of the plane wave impinged on the array.

The directional properties of the radiation pattern are usually described by the power pattern, which originates in the Poynting vector **S** measured in Watts/m^2, that gives the angular dependence of power on the variation of (θ, ϕ) of the originating radiation source. The instantaneous value of **S** describes the magnitude and direction of the power/m^2 that is parallel to the *xy* plane, and is derived from the cross product of the electric field density (**E**), and the complex conjugate magnetic field (**H***) vectors, expressed in V/m and A/m units respectively. The direction then of S (or the power) is perpendicular to the *xy* plane (E_x,H_y plane). Hence, for z-directed sources the normalized power pattern is (2).

$$P(\theta,\phi) = \left|F(\theta,\phi)\right|^2 \quad (2)$$

It could be easily shown that when the radiation pattern $F(\theta,\phi)$ is expressed in volts, (not normalized), then the power expressed in dB units is the same as the radiation pattern in dB. i.e. $P(\theta,\phi)_{dB} = \left|F(\theta,\phi)\right|_{dB}$. The radiated power $P(\theta,\phi)$ of the beam in (3) is related to the antenna directivity $G(\theta,\phi)$ in (4) by means of the power density $U(\theta,\phi)$ which is the power per unit solid angle in the direction (θ, ϕ) expressed in Watts/(rad)^2.

$$P(\theta,\phi) = \int_{\phi=0}^{2\pi}\int_{\theta=0}^{\pi} U(\theta,\phi)\sin\theta d\theta d\phi \quad (3)$$

$$G(\theta,\phi) = \eta \frac{U(\theta,\phi)}{U_{avg}} \quad (4)$$

where: η is the antenna efficiency factor, and U_{avg} is the average power density $P(\theta,\phi)/4\pi$ of an isotropic antenna. The antenna gain is then expressed in dBi rather than in dB. For the ideal case where there are no losses at the antenna and perfect

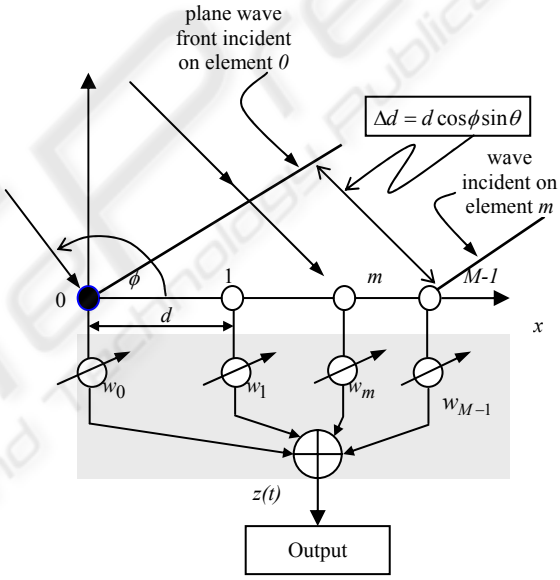

Figure 4: Linear array - UE ESLA

impedance matching, $\eta = 1$ and the expression in (4) is termed the gain, i.e. the gain is related to the directivity of the antenna only by the efficiency factor η. In our model, we assume, $\eta = 1$ and that gain and directivity are interchangeable.

Though we used the antenna synthesis parameters to derive at the radiation patterns, we chose not to use the Dolph-Chebyshev synthesis method that deals with low sidelobes and narrow main beam design, since the solution to those polynomials depend only on the number of elements in the array and not on the interelement spacing, which is pivotal to the array design in this work.

We designed a linear equally spaced antenna array, consisting of 8 elements along the *x*-axis with interelement spacing *d* as shown in Figure 4. We assumed the elements of the array to be identical, uniformly excited (UE), and that the array factor $f(\theta,\phi)$ represents the sum over the currents for each element weighted by the spatial phase delay w_m from each element to the far-field point (Stutzman & Thiele 1998). The UE equally spaced linear array (ESLA) in Figure 4 attempts to capture Figure 3-3 from Liberti & Rappaport (1999, Pg 85) that describes the basis for the design used in this work. As shown in Figure 4, the impinged plane wave arriving from an angle (θ,ϕ) relative to the x-axis will travel an additional distance $\Delta d = d\cos\phi \sin\theta$ before arriving at element m, relative to the element at the origin. The difference

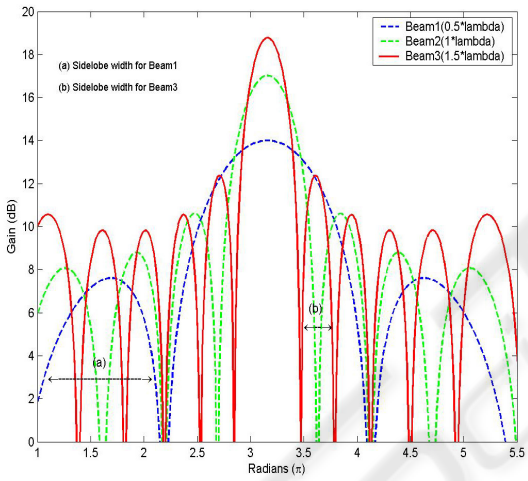

Figure 5: Linear array with three variants on the interelement spacing

in phase $\Delta\xi_m$ between the signal component on element *m* and the element at the origin is (5).

$$\Delta\xi_m = \beta\Delta d = \beta(x_m\cos\phi\sin\theta + y_m\sin\phi\sin\theta + z_m\cos\theta) \quad (5)$$

where: β is the phase propagation factor and is equal to $2\pi/\lambda$.

Assuming the elevation angle θ is equal to $\pi/2$, and substituting $x_m = m\Delta d$ in (5), the received signal $x_m(t)$ at antenna element *m* along the x-axis is (6) without taking noise/interference into consideration, and the output of the array *z(t)* is (7). In vector notation the left side of (7) is represented in (8).

$$\begin{aligned} x_m(t) &= s_m(t) \\ &= As(t)e^{-j\beta m\Delta d} \\ &= As(t)e^{-j\beta md\cos\phi\sin\theta} \end{aligned} \quad (6)$$

$$z(t) = \sum_{m=0}^{M-1} w_m x_m(t) = As(t)\sum_{m=0}^{M-1} w_m e^{-j\beta md\cos\phi\sin\theta} = As(t)f(\theta,\phi) \quad (7)$$

where: A is an arbitrary gain constant, *s(t)* is the baseband complex envelope representing the modulation of the plane wave, $f(\theta,\phi)$ is the array factor, and w_m the weighting element associated with the mth branch of the array where $w_m = e^{j\beta md\cos\phi}$.

$$\mathbf{z} = \mathbf{w}^H\mathbf{x} \quad (8)$$

where: $\mathbf{x} = [x_0, x_1, x_2, ..., x_{M-1}]$, $\mathbf{w}^H = ([w_0, w_1, ..., w_{M-1}]^T)^*$, and H, the Hermitian operator is the complex conjugate (*) of the transpose vector w^T.

The UE-ESLA used in the design for this study represents three configurations based on

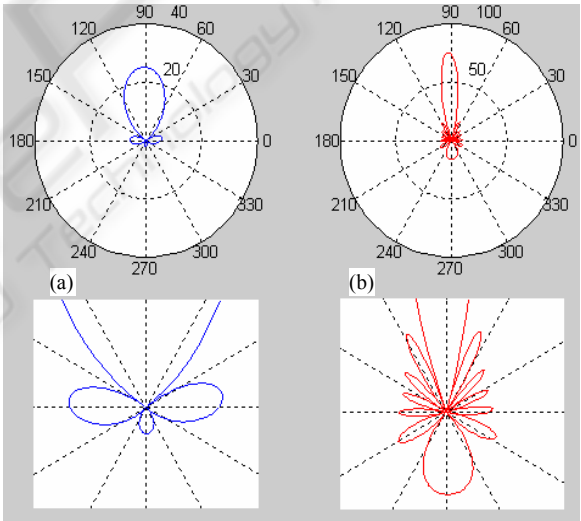

Figure 6: Polar representation of patterns for interelement spacing (a) d1 (b) d3

interelement spacing: $d1 = 0.5\lambda$, $d2 = 1\lambda$, and $d3 = 1.5\lambda$, corresponding to Beam1, Beam2, and Beam3 respectively in Figure 5, which shows the gain as a function of the interelement spacing. By adjusting the set of weights w_m, it is possible to direct the boresight (the direction of maximum radiated power in the main beam) of the array pattern in any desired direction of θ,ϕ. As shown in Figure 5, Beam1 represented by the antenna pattern with an interelement spacing $d1 = 0.5\lambda$, has a boresight of 14.024dBi. Beam2 (green) - $d2 = 1\lambda$, a

boresight of 17.013dBi, and Beam3 (red) where $d3 = 1.5\lambda$ has the maximum gain in its boresight of 18.774dBi. It is readily seen in Figure 5 that the larger the interelement spacing, the higher the gain and sidelobe peaks. Thus for *d3*, the gain of the main beam pattern (boresight) and its sidelobes are the highest (Figure 5(b)), while for *d1*, the gain of the main lobe and its sidelobes are the lowest (Figure 5(a)). To quantify the beam width we used the metric Half Power Beamwidth (HPBW), which describes the angular width between the points on the main lobe that are 3dB below the boresight. The HPBWs for Beam1, 2 and 3 are 106^o, 52^o, 34^o, respectively. Another metric of interest that describes the characteristics of the radiation pattern is the sidelobe level (SLL) and is defined as the ratio between the absolute maximum value of the largest sidelobe to the absolute maximum value of the main lobe (Stutzman & Thiele 1998).

It is readily seen that as the interelement spacing increases the HPBW decreases, and the sidelobe peak increases. This will have profound implications on the throughput performance, as we will see later in Section 5. It is interesting to note that the SLL for all three interelement spacing is nearly the same (in the vicinity of *minus* 12.8dB) in spite of the fact that the sidelobe peak of Beam1 (Figure5) is significantly less than that of Beam3. Therefore, one may assume that Beam3 would be more vulnerable to interference than Beam1 although the SLL for both beams is the same. This fact is more pronounced in Figure 6. Both Figures 6a and 6b are the polar representations of Beam1 and Beam3 respectively with an enlargement view of their sidelobes immediately below. We distinctly see that as the interelement spacing increased the number of sidelobes increased, and the gain of the backlobe (Figure 6b) increased significantly, presenting a higher risk with respect to interference. The extra main lobes formed with large interelement spacing are referred to as grating lobes.

4 MAXIMIZING THE SINR IN FADING CHANNELS

The mobile radio channel in ad hoc networks deviates considerably from the stationary additive white Gaussian noise (AWGN) channel due to continuous variations in the environment, motion of surrounding objects, and the mobility of the device itself. In such an environment, the transmitted signal arrives at the receiver from different paths (multipath) caused by its wave scattering off of building and objects, which results in delays and attenuation of the received signal at the antenna elements. This phenomenon known as fading is used in wireless communication to describe the fluctuation in the amplitude and phase of a radio signal over a time period or travel distance. Fading can lead to significant degradation in the reception of the desired signal or in the signal to noise plus interference ratio SINR, resulting in unacceptable levels of throughput in the network. In non-frequency selective fading (or flat fading) channels where the signal bandwidth is less than the channel bandwidth, variations in amplitude of the multipath signals arriving at the receiver may be expressed statistically in terms of a Rayleigh probability distribution function. It has been shown (Furman, Hammers & Gerla 2003) that with mobility the signal strength of the envelope of the received signal has deep fades that may dip as low as –10dB, which is significantly below the threshold when compared with the no-mobility case. These flat-fading results may require up to 20 to 30dB more transmitter power to acquire the equivalent bit error rate (BER) performance of that obtained in an AWGN channel.

To meet the increased demand of SINR that will result in increased throughput, directional antennas may well be the solution as discussed in Section 2. To maximize the SINR analytically in a fading channel, we considered two basic configurations as a function of interelement spacing. The first configuration is associated with a fraction of a wavelength interelement spacing (e.g. 0.5λ) as in Beam1, and is usually considered an adaptive array. An adaptive array employs small (fractional λ s) interelement spacing to avoid grating lobes and relies on various algorithms (Monzingo & Miller 1980) to dynamically adjust the weights w_m associated with each branch of the array in Figure 4. Some of these algorithms may also be used to generate optimum weights in fixed beam arrays, consistent with the weights used in this work. The second configuration assigns interelement spacing in multiplies of λ. This configuration corresponds to Beam2 and Beam3 in our design, and is usually referred to as 'combining methods' in antenna diversity. In the second configuration, the weights w_m assigned to each of the branches are predefined.

To determine the optimum weight assignment that will maximize the SINR in a fading channel, we first expand on the description of the signal in (6) to include the interference and noise $n_m(t)$ at each of the antenna elements of the receiver (9).

$$x_m(t) = s_m(t) + n_m(t) \tag{9}$$

The output *z(t)* of the array then comprises of two components the desired signal z_s, and the noise/interference component z_n (10), and is represented in (11) vector form.

$$\begin{aligned} z_s &= \sum_{m=0}^{M-1} w_m s_m \\ z_n &= \sum_{m=0}^{M-1} w_m n_m \end{aligned} \tag{10}$$

$$\begin{aligned} z_s &= \mathbf{W}^T \mathbf{S}_d \\ z_n &= \mathbf{W}^T \mathbf{N} \end{aligned} \tag{11}$$

where: $\mathbf{S}_d = [s_0, s_1, s_{2,\ldots,} s_{M-1}]^T$ and $\mathbf{N} = [n_0, n_1, n_{2,\ldots,} n_{M-1}]^T$ are the desired signal and the noise associated with the antenna elements respectively.

The average noise power is then (12).

$$\begin{aligned} &P_n = E[|z_n|^2] = E[\mathbf{w}^H \mathbf{N}\mathbf{N}^T \mathbf{w}] = \mathbf{w}^H E[\mathbf{N}\mathbf{N}^T]\mathbf{w} \\ &or \\ &P_n = \mathbf{w}^H \mathbf{R}_n \mathbf{w} \end{aligned} \tag{12}$$

where: R_n is the correlation matrix of the noise defined by $E[n(t)n(t)^H]$.

The noise correlation matrix R_n for the 8-element linear array is then (13), where $(\bullet)$ represents convolution, and the *bars* above each entry within the matrix represent average.

$$R_n = \begin{bmatrix} \overline{n_1(t) \bullet n_1(t)} & \overline{n_1(t) \bullet n_2(t)} & \cdots & \overline{n(t) \bullet n_8(t)} \\ \overline{n_2(t) \bullet n_1(t)} & \overline{n_2(t) \bullet n_2(t)} & \cdots & \overline{n_2(t) \bullet n_8(t)} \\ \vdots & \vdots & \cdots & \vdots \\ \overline{n_8(t) \bullet n_1(t)} & \overline{n_8(t) \bullet n_2(t)} & \cdots & \overline{n_8(t) \bullet n_8(t)} \end{bmatrix} \tag{13}$$

The computation of R_n in (13) is significantly simplified by transforming the convolution in the time domain into multiplication of the individual transforms in the frequency domain. Similarly, an expression for the average signal output power may be expressed in (14).

$$P_s = \mathbf{w}^H \mathbf{R}_s \mathbf{w} \tag{14}$$

where: R_s is the correlation matrix (or the covariance matrix with zero mean) of the desired signal.

The cost function (15) then is defined as the ratio of the average noise power to the average (desired) signal power (14).

$$J(w) = \frac{\mathbf{w}^H \mathbf{R}_n \mathbf{w}}{\mathbf{w}^H \mathbf{R}_s \mathbf{w}} \tag{15}$$

To minimize the cost function in (15), we take the derivative of the numerator and set it to zero, i.e. we use the gradient operator ∇ on $(\mathbf{w}^H \mathbf{R}_n \mathbf{w})$ or $\nabla(\mathbf{w}^H \mathbf{R}_n \mathbf{w})$. As a sideline, it should be noted that since the diagonal elements of the noise correlation matrix in (13) are real, the matrix is Hermetian, which implies that a matrix $\mathbf{A}$ exists for which $\mathbf{A}^H \mathbf{R}_n \mathbf{A} = \mathbf{I}$, where $\mathbf{I}$ is an identity matrix. This matrix identity is essential in order to derive at the solution for the cost-function in (15). The optimal solution to minimizing (15) is (16) (Monzingo & Miller 1980).

$$\mathbf{R}_n^{-1} \mathbf{R}_s \mathbf{w} = \rho_{\max} \mathbf{w} \tag{16}$$

where: $\rho_{\max}$ is the maximum eigenvalue of the signal covariance matrix $\mathbf{R}_s$. To find the eigenvalues that satisfy (16) we expand the determinant $|R_n^{-1} R_s - \rho I|$.

Both configurations described in this section use complex weights to adjust the incoming signal from each antenna element, which are then combined (summed) into a signal directed to the receiver's detector. For this study, we assumed that the weights associated with each of the elements are fixed and provide equal gain in all directions. The weights derived to maximize the SINR were varied only as a function of the interelement spacing *d*.

5 NETWORK SIMULATION AND RESULTS

To perform the network simulation for this study we used the QualNet simulator (SNT, 2002), which is a discrete event high performance networking research tool for various configurations of wired and wireless networks. QualNet supports directional antennas and

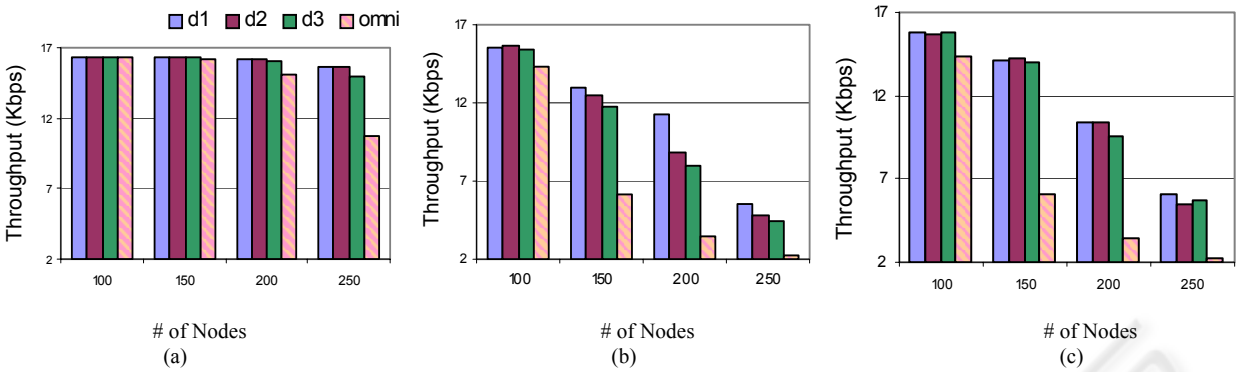

Figure 7: Throughput performance as a function of network density (a) AWGN channel (b) Fading channel (c) Null steering (ns) in a fading channel

has the built-in capability to steer the radiation pattern of the antenna array in the direction of communication.

The ad hoc network for the simulation was based on the IEEE802.11b standard (IEEE, 2000), and the environment for the simulation comprised of a terrain 1600x1600m with 100, 150, 200, and 250 nodes randomly distributed. Experiments were performed with the assumption that the nodes are mobile, and we used the Random Waypoint mobility algorithm to implement mobility (with speeds 0 to 10m/s, and 0 pause time). The ad hoc on-demand vector distance (AODV) routing protocol was used in all the scenarios of the simulation. We used differential quadrature pulse shift keying (DQPSK) modulation, which adjusts the carrier and bit timing to produce the in-phase (I) and quadrature (Q) components of the transmitted signal. The minimum threshold for the receiver was set at -81dBm and its sensitivity at -91.0dBm. The carrier frequency used was f_c=2.4GHz with a data payload of 2Mbps. Traffic was generated using a constant bit rate (CBR) generator with a ratio of 1:5 sessions per CBR. Data transfer was at 4 packets/s and each packet was set at 512 bytes in length. The results obtained from the network simulation represent an average of 5 runs with random seeds in the configurations described above for each of the three radiation patterns derived from the interelement spacing, in reference to an omnidirectional antenna. In addition, we repeated the entire set of simulation described above with null-steering by suppressing the sidelobes for each the three patterns. All the simulation experiments were performed for both AWGN and Rayleigh (fading) channels. The distributed coordination function (DCF) of the IEEE 802.11 (IEEE, 1999) MAC protocol was used to implement the CSMA/CA protocol. A refinement to this access method implements RTS, to further minimize collisions prior to data transmission. The additional overhead however, of the RTS mechanism may not always be justified (Gerla, 1997). Accordingly, the MAC protocol was modified to disabled the RTS in order to reduce bandwidth overhead.

Two scenarios, low-density and high-density are presented (we define density as #nodes/area). The low-density addresses the performance for 100-150 nodes, and the high-density for 200-250 nodes. The results obtained from the simulation are shown in Figure 7(a)-(c). For the AWGN channel (Figure 7(a)) the performance difference between the omnidirectional antenna and the arrays in the low-density case was less than 1% (on the average). In the high-density case, the performance with the arrays was at least 22% better than with the omnidirectional antenna. For the fading scenario in Figure 7(b), the performance difference between the omnidirectional antenna and the arrays in the low-density scenario increased significantly and was computed to be 37% (compared to the 1% above), and 152% (compared to the 22% above) for the high-density. Figure 7(c) is an extension of the simulation represented by Figure 7(b), with the exception that in this case we used null-steering to improve performance. With null steering, the performance increased for all three variants of interelement spacing. The performance improvement in the fading channel with null-steering for the low-density scenario was on the average 46%, where as for high-density the improvement was

approximately 180% with respect to the performance of an omnidirectional antenna.

Figure 8 shows the relative performance as a function of interelement spacing in both low and high density for channel conditions with no fading - *'nF'*, with fading - *'F'*, and with fading and null-steering - *'F_ns'*. It is clearly seen from Figure 8, that the d1 interelement spacing in all the experiments attained the maximum performance. This fact is interesting since the gain of the array with *d2* and *d3* interelement spacing is greater than that of *d1* (Figure 5), yet the performance was less, which is contrary to an intuitive prediction.

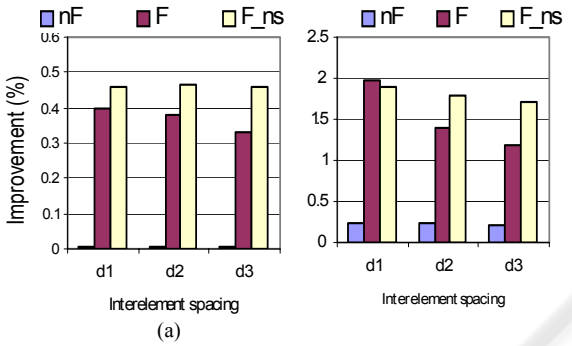

Figure 8: The relative throughput performance improvement as a function of interelement spacing (a) Low density (b) High density

6 SUMMARY AND CONCLUSIONS

In this work, we discussed the benefits of directional antennas in ad hoc networks and the necessity to supplement prior work with accurate directional antenna design models. We used antenna synthesis to guide the design of the antenna arrays, and in Section 4 described an analytical approach to determine the optimum weight w_m that maximizes the SINR. The radiation patterns from the design of the linear array with the three variants of interelement spacing *(d1*, *d2*, and *d3)* were then used in the network simulation to quantify the effects of interelement spacing on throughput performance for both low and high densities network scenarios. In each scenario, we compared the throughput performance in an AWGN channel, a fading channel (Rayleigh fading), and finally in a fading channel utilizing null-steering.

We conclude that regardless of the interelement spacing in the linear array, the throughput performance in the network increased compared to that of an omnidirectional antenna. The effects of the interelement spacing on the performance of the network were not necessarily predictable, and were in fact the case where '*less is more*'. The results show that Beam1 (smallest interelement spacing *d1*) with the lowest gain, interestingly performed the best and resulted in a higher throughput performance, while Beam3 (*d3* interelement spacing), with the most gain consistently produced the lowest results. These results are attributed to (a) the mobility of the nodes, and (b) amplification of the interference in the sidelobes. As the beam became narrower (more gain, larger interelement spacing, and lower HPBW), the node due to mobility drifted out of the main beam area faster than with the wider beam, thereby producing inferior results compared to that of the wider beam with lower gain. Further, the amplification of interference was greater as the interelement spacing increased because the grating lobes increased and the peak of the sidelobes increased, leaving Beam1 to perform superior with respect to interference. Finally, we conclude that in an AWGN channel the use of antenna arrays were not meaningful in the low-density network scenario while for a realistic channel model (a Rayleigh channel), antenna arrays can substantially increase network performance and in some cases, the increase may be as high as 197%.

REFERENCES

Blogh J. S., and Hanzo, L., 2002. *Third Generation Systems and Intelligent Wireless Networking*, John Wiley & Sons, Ltd, New York.

Furman, S., Hammers, D. E., and Gerla, M., 2003. "Optimum Combining for Rapidly Fading Channels in Ad Hoc Networks", *SCI'03 Proc. of The 7th World Multiconference on Systemics, Cybernetics and Informatics* vol. III, July 27-30, Orlando, pp 49-54.

Gerla, M. and Talucci, F., 1997. "MACA-BI (MACA By Invitation) A Wireless MAC Protocol for High Speed ad hoc Networking", *Universal Personal Communication Records, IEEE*, 6th International Conference, vol. 2, pp. 913-917.

Hadzi-Velkov, Z., and Gavrilovska, L., 1999. "Influence of Burst Noise Channel and Hidden Terminals over the IEEE 802.11 Wireless LANs", *VTS'99, Vehicular*

Technology Conference, *IEEE*, 50th Conference, vol.5, pp. 2641-2945.

IEEE Std. 802.11, 1999. "Wireless LAN Medium Access Control (MAC) and Physical Layer (PHY) Specifications", *The Institute of Electrical and Electronics Engineers, Inc*., ISBN 0-7381-1658-0.

IEEE Std. 802.11b-1999, 2000. "Wireless LAN Medium Access Control (MAC) and Physical Layer (PHY) Specifications: Higher-Speed Physical Layer Extension in the 2.4 GHz Band", *The Institute of Electrical and Electronics Engineers, Inc*., ISBN 0-7381-1811-7.

Khurana, S., Kahol, A., and Jayasumana, A. P., 1998. "Effect of Hidden Terminals on the Performance of IEEE 802.11 MAC Protocol", *LCN'98, Local Computer Networks Proc.* 23rd, pp. 12-20.

Ko, Y-B., Shankarkumar, V., and Vaidyn, N.H., 2000. "Medium Access Control Protocols using Directional Antennas in Ad Hoc Networks", *IEEE INFOCOM*, pp 13-21.

Liberty, J.C. Jr., and Rappaport, T.S., 1999. *Smart Antennas for Wireless Communications: IS-95 and Third Generation CDMA Applications*, Prentice Hall, Upper Saddle River, NJ.

Monzingo, R.A., and Miller, T.W., 1980. *Introduction to Adaptive Arrays*, John Wiley & Sons, New York.

Nasipuri, A., et al, 2000. "A MAC Protocol for Mobile Ad Hoc Networks Using Directional Antennas", *WCNC'00,Wireless Communications and Networking Conference, IEEE*, vol.3, pp. 1214-1219.

Peterson, L. L., and Davie, B. S., 2000. *Computer Networks A Systems Approach*, Morgan Kaufmann Publishers, 2nd edition, San Francisco.

Ramanathan, R., 2001. "On the performance of Ad Hoc Networks with Beamforming Antennas", *MOBIHOC'01, International Symposium on Mobile Ad Hoc Networking & Computing*, *Proc.* ACM, pp. 95-105.

Sanchez, M., Giles, T., and Zander, J., 2001.ACSMA/CA with Beam Forming Antennas in Multi-hop Packet Radio@, *Radio Communication Systems, Proc. of the Swedish Workshop on Wireless Ad-hoc Networks*.

SNT, 2002. "QualNet Simulator & User's Manual", *Scalable Network Technologies, Inc.,* Los Angeles.

Stutzman, W. L., and Thiele, G. A., 1998. *Antenna Theory and Design*, John Wiley & Sons, Inc., 2nd edition, NY.